Thermochromic Core–Shell Nanofibers Fabricated by Melt Coaxial Electrospinning

Fengyu Li,[1] Yong Zhao,[1] Sen Wang,[1,2] Dong Han,[3] Lei Jiang,[1] Yanlin Song[1]

[1]*Key Laboratory of Organic Solids, Institute of Chemistry, Chinese Academy of Sciences, Beijing 100190, People's Republic of China*
[2]*School of Material Science and Engineering Beihang University, Beijing 100191, People's Republic of China*
[3]*National Center for Nanoscience and Technology, Beijing 100190, People's Republic of China*

Received 16 December 2007; accepted 7 October 2008
DOI 10.1002/app.29384
Published online 22 December 2008 in Wiley InterScience (www.interscience.wiley.com).

ABSTRACT: Microcapsule/nanocapsule and encapsulation techniques have great potential for devices of functional materials. Also, electrospinning has attracted great attention for the fabrication of microstructures and nanostructures. The fluidity after melting limits the application of phase-transformation thermochromic materials. In this study, with the melt coaxial electrospinning technique, a phase-transformation thermochromic material was encapsulated in poly(methyl methacrylate) nanofibers. A device of this phase-transformation thermochromic material was realized. With a poly(methyl methacrylate) shell with good optical transmission and a thermoresponsive core made of crystal violet lactone, bisphenol A, and 1-tetradecanol core, the fibers had good thermal energy management, fluorescent thermochromism, and reversibility. The fabrication of thermochromic core–shell nanofibers has further potential in the preparation of temperature sensors with good fluorescence signals and body-temperature calefactive materials with intelligent thermal energy absorption, retention, and release. © 2008 Wiley Periodicals, Inc. J Appl Polym Sci 112: 269–274, 2009

Key words: core-shell polymers; fibers; nanotechnology; phase behavior; thermal properties

INTRODUCTION

The combination of stimuli-responsive compounds with microstructures and nanostructures could generate many good functional materials, and this is drawing much attention to the great potential of smart materials and devices.[1–4] With the development of the electrospinning technique and applications of various stimuli-responsive materials, scientists have fabricated various functional and stimuli-responsive fibers and particles.[5–22] Phase-change thermochromic materials (PCTMs) have attracted much attention for their phase-transformation reversibility and energy-storage and management properties.[23,24] However, because of the fluidity of phase-change materials after melting, pure PCTMs cannot be fixed, and this limits their practical applications. Using the melt coaxial electrospinning technique, Xia's group[25] successfully fabricated phase-change materials encapsulated by core–shell TiO_2–polyvinylpyrrolidone nanofibers. Therefore, the combination of melt coaxial electrospinning and PCTMs, with PCTMs encapsulated in core–shell nanofibers, has further potential in thermal energy management and sensors.

Crystal violet lactone (CVL) as a dye and bisphenol A as a developer, mixed with a fatty alcohol or fatty acid, compose a traditional PCTM system[26–28] (Scheme 1). This material system has stable thermochromic properties. In particular, the thermochromic temperature can be adjusted by changes in the fatty alcohol or fatty acid. The phase-change temperature of 1-tetradecanol is 37–39°C, which is the body temperature of a human being. With potential for intelligent sensors and devices made of body-temperature materials, CVL, bisphenol A, and 1-tetradecanol can compose a body-temperature PCTM system. As shown in Figure 1, the CVL–bisphenol A–1-tetradecanol mixture system (CBT) has an obvious absorption and release process at the melting point of 37–39°C, and there is a fluorescent change at its phase-change temperature. Therefore, the encapsulation of CBT is promising for PCTM applications in body-temperature thermal materials and thermoresponsive sensors. Here, using melt coaxial electrospinning, we encapsulated PCTM CBT in poly (methyl methacrylate) (PMMA) fibers and fabricated core–shell nanofibers. With a PMMA shell with good optical transmission properties, these fibers were expected to have body-temperature thermal energy management, thermochromism, and fluorescence properties.

Correspondence to: Y. Song (ylsong@iccas.ac.cn).
Contract grant sponsor: National Science Foundation of China; contract grant numbers: 50625312, 60601027, 20421101, U0634004.
Contract grant sponsor: 973 Program; contract grant numbers: 2006CB806200, 2006CB932100.
Contract grant sponsor: Chinese Academy of Sciences.

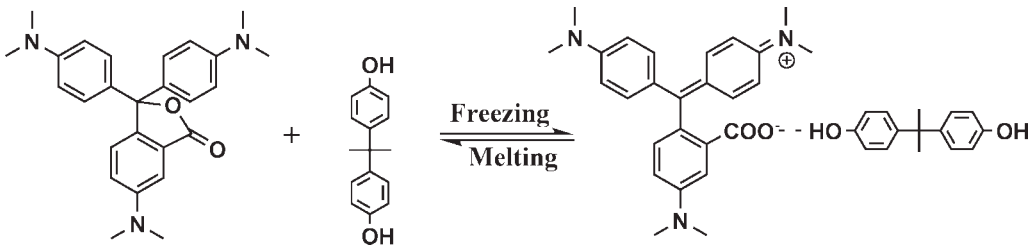

Scheme 1 CVL and bisphenol A chromism in the phase-change process.

EXPERIMENTAL

Preparation of the solution and electrospinning setup

CVL (Aldrich), bisphenol A (Aldrich), 1-tetradecanol (analytical reagent, Beijing, China), PMMA (weight-average molecular weight ≈ 120,000; Aldrich), and dimethylformamide (DMF; analytical reagent, Beijing, China) were used as received. PMMA was dissolved in DMF, and a DMF solution of PMMA was prepared (10–15 wt %). CVL, bisphenol A, and 1-tetradecanol were mixed in a 1 : 2 : 20 weight ratio.

The melt coaxial electrospinning experimental setup is shown in Figure 2. A heating system was appended to the conventional coaxial electrospinning setup.[11] It provided a thermal atmosphere for the whole loaded system of the electrospinning setup. A high electric potential was supplied by a Spellman SL50P60 high-voltage generator (USA). The flow rate of the solution was controlled with an NE-1600 syringe pump (New Era, United States). The heating mantle was constructed of a glass thermal tube as the insulating frame and heating tapes with a controllable electrical source. The outer and inner dope load setup was constructed with two injectors and needles with different diameters.

Electrospinning

The PMMA solution in DMF (10–15 wt %) was loaded in the outer syringe, and the melting CBT was loaded in the inner syringe. The heating mantle was set at 45°C and held the whole loaded set above 40°C to keep the inner dopes flowing fluidly. The inner dope of the melting CBT mixture was controlled with a flow rate of 0.2–1.0 mL/h by a syringe pump. The inner nozzle was connected to the cathode of the high-voltage generator, and a metallic

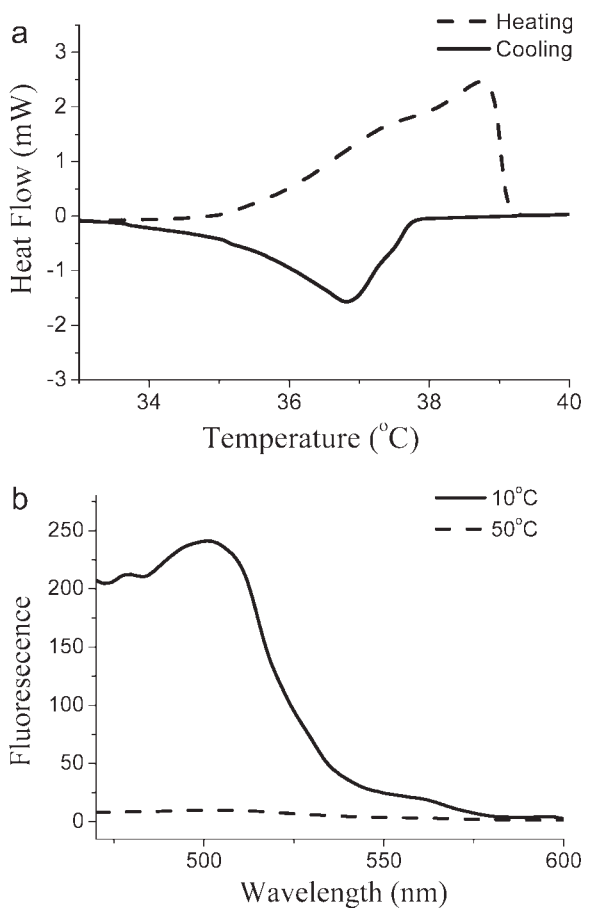

Figure 1 (a) DSC cycle curve of CBT and (b) fluorescence spectra of a CBT film at (—) 10 and (- - -) 50°C.

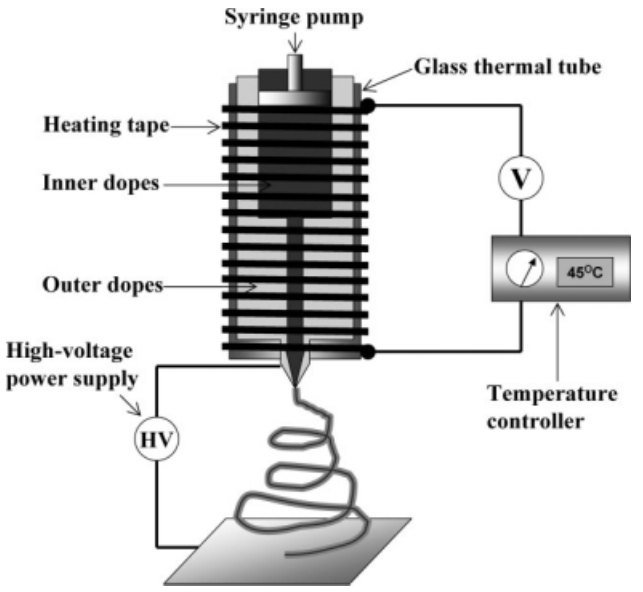

Figure 2 Melt coaxial electrospinning setup used for fabricating PMMA nanofibers loaded with PCTM CBT.

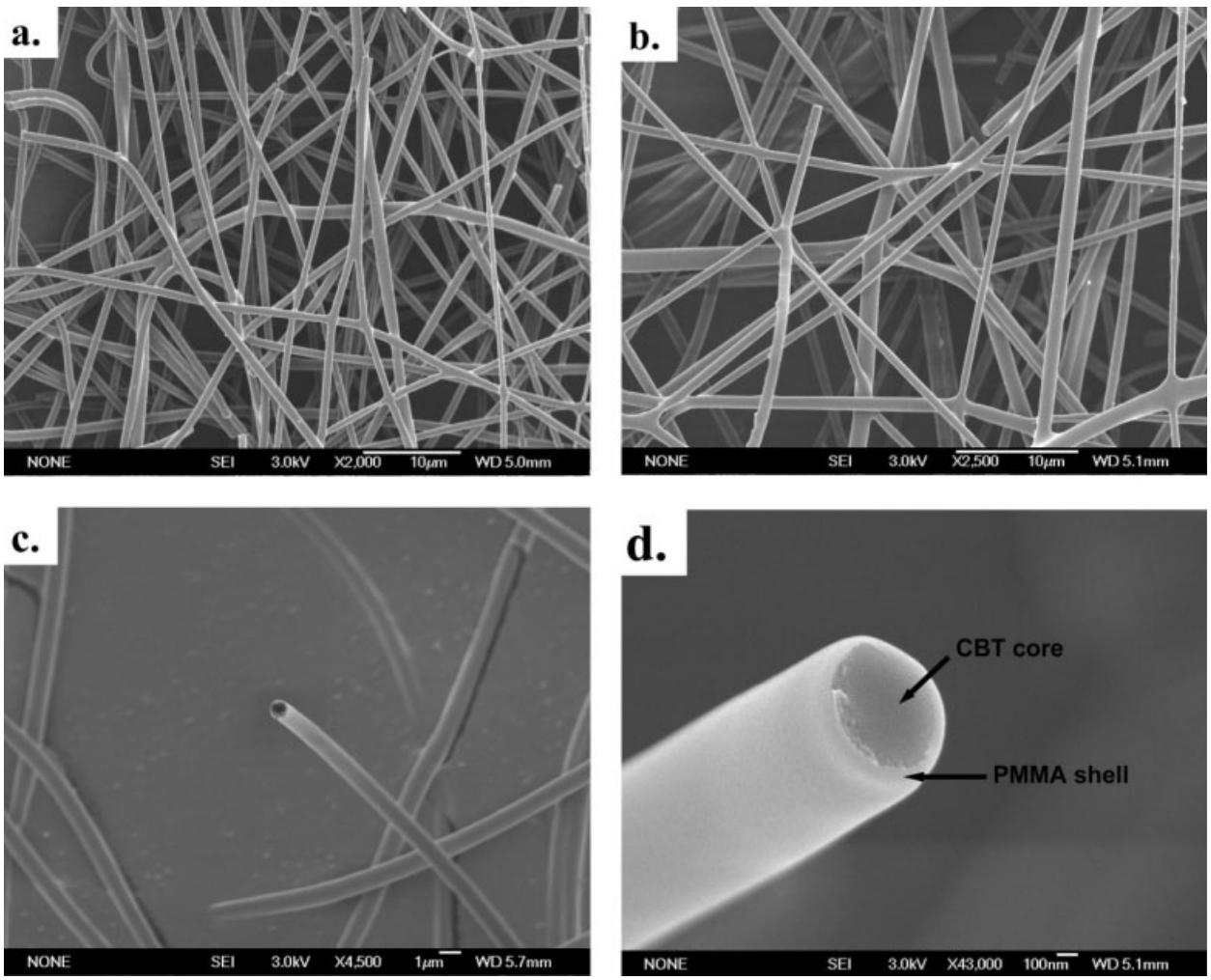

Figure 3 Electron microscopy images of core–shell PMMA nanofibers loaded with CBT: (a,b) SEM images of the fibers in a wide area and (c,d) SEM images of lateral sections of the fibers.

plate covered with a piece of aluminum foil was connected to the anode as a collecting substrate. The voltage was set at 20–30 kV, and the work distance was 15–25 cm. In our experiment, the whole thermal atmosphere of the loaded system was more beneficial for preventing the inner dope from freezing by jamming of the needle, and this ensured that the melted CBT would be encapsulated within the fibers.

Characterization

Scanning electron microscopy (SEM) images were taken with a JEOL FE-SEM 6700F microscope (Japan). Transmission electron microscopy (TEM) image was obtained with a JEOL JEM-2010 microscope. Fluorescent characterization was carried out with a Hitachi F-4500 fluorescence spectrophotometer (Japan) and a YoKoGaWa CSU10 confocal scanner unit fluorescent microscope (Japan). Differential scanning calorimetry (DSC) measurements were conducted on a PerkinElmer DSC-7 (USA) and performed on 2.0–5.0 mg samples in Al pans. For DSC, a 2°C/min scanning rate was used.

RESULTS AND DISCUSSION

After a fluid melt coaxial electrospinning process, PMMA fibers with PCTM CBT encapsulation in a large area were fabricated. SEM images [Fig. 3(a,b)] show that the fibers had smooth surfaces and an average diameter of 500 nm to 2 μm. In other SEM images [Fig. 3(c,d)], the core–shell lateral sections of the fibers can be seen. The TEM image in Figure 4 shows the core–shell structure of the fibers more clearly, demonstrating that CBT was encapsulated in the PMMA fibers. The clear interface of the CBT core and PMMA shell means that the PCTM CBT was phase-separated from the PMMA polymer. Thus, the phase-transformation property of the PCTMs was free and uninfluenced. In other words,

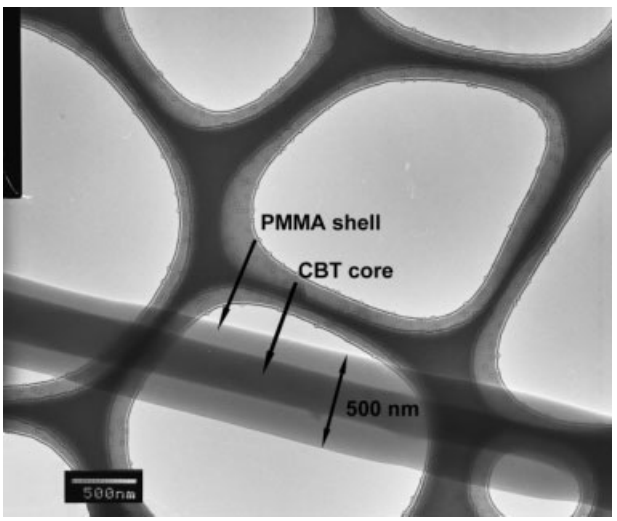

Figure 4 TEM image of the fibers.

CBT was encapsulated in nanodimensional PMMA fibers with a clear core–shell nanostructure.

The DSC experiment proved the phase-transformation property of the as-fabricated compound fibers [Fig. 5(a)]. The CBT–PMMA nanofibers had an obvious absorption and release process in the DSC measurement cycle. Therefore, the nanostructure of the fibers did not affect the phase transformation of the PCTMs. With a larger heating surface area by microsize encapsulation, the CBT–PMMA nanofibers had a more sensitive phase-transformation behavior than a bulk CBT mixture.[25] As microsize and nanosize materials, the fibers had average core diameters of 200–400 nm and average shell thicknesses of 200–500 nm. The wavelength of visible light was around 400–800 nm. In the scale ($0.1 <$ average diameter/wavelength < 10), there was a great Mie light scattering phenomenon.[29,30] The high scattering coefficient of Mie scattering meant that the core–shell nanofibers could not show the blue reflectance color of CVL in the bulk CBT thermochromic process.[31–33] Then, the fluorescent property was studied for a film of the nanofibers on a quartz plate. Figure 5(b) shows the fluorescence spectra of the fibers. There is a fluorescent emission peak at

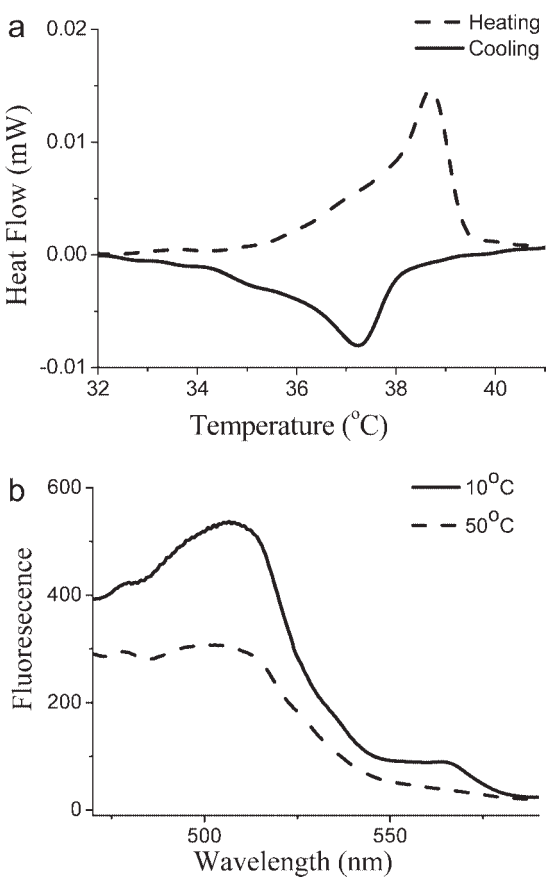

Figure 5 (a) DSC cycle curve of CBT–PMMA nanofibers and (b) fluorescence spectra of a CBT–PMMA nanofiber film at (—) 10 and (- - -) 50°C.

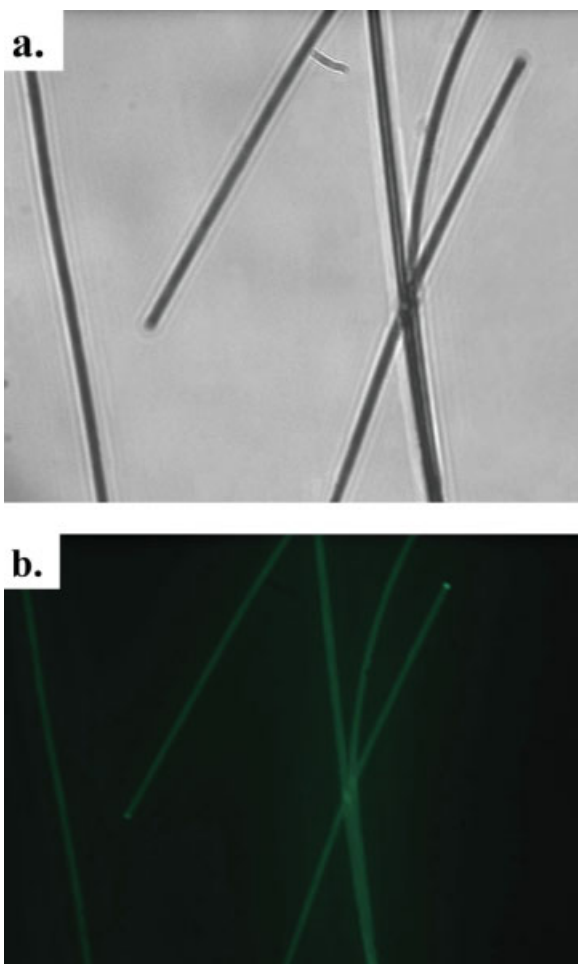

Figure 6 (a) Optical and (b) fluorescent images of CBT–PMMA fibers under a fluorescence microscope. [Color figure can be viewed in the online issue, which is available at www.interscience.wiley.com.]

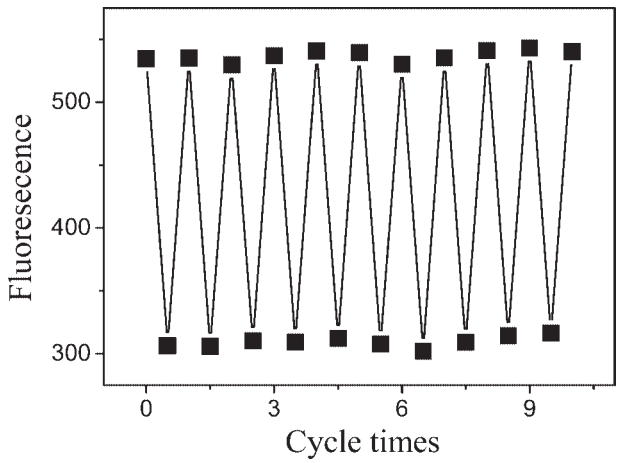

Figure 7 Results of a thermochromic cycle reversibility experiment with CBT–PMMA nanofiber films. In each cycle, the fluorescence emission of the samples at the wavelength of 503 nm was monitored at 10 and 50°C.

503 nm, which is the characteristic fluorescence emission of CVL in the CBT system. At the freezing state of CBT at 10°C, the fibers had strong fluorescence emissions. With the temperature increased to 50°C, the emission intensity of the fibers greatly decreased. When the temperature was reduced to 10°C, the emission intensity reverted again. The fluorescence change in the fibers in the heating–cooling process showed thermochromism similar to that of CBT. Figure 6 shows a clear fluorescent signal of the thermochromic nanofibers with a transparent outer shell of PMMA. This indicates the potential of the fibers for thermoresponsive sensors. Here, residual fluorescence can be seen in the thermochromism of the fibers above the melting temperature of CBT because the fast flow during the electrospinning process mixed some CVL into the PMMA shell, and this resulted in the residual fluorescence.

The fluidity after melting is the main limiting factor of practical applications of PCTMs. The encapsulation of PCTMs in a micromatrix or nanomatrix can fix PCTMs and lead to phase-transformation reversibly performed in a fixed region. Therefore, with good reversibility of the phase transformation of PCTMs, PCTM devices will have good reversibility. Then, thermochromic reversibility cycle experiments of a CBT–PMMA fiber film were investigated (Fig. 7). The maximum fluorescent emission at 503 nm of the fiber film was monitored. After 10 heating–cooling cycles between 10 and 50°C, there was no essential loss of the fluorescent characteristics during repeated thermochromism processes. This proved that the CBT–PMMA core–shell nanofibers had good fluorescence thermochromic reversibility. The encapsulation of CBT in PMMA nanofibers could lead to devices and practical applications of PCTM CBT.

CONCLUSIONS

With melt coaxial electrospinning, thermochromic phase-change nanofibers with a transparent PMMA shell and a PCTM CBT core were successfully fabricated. With body-temperature phase-change materials and 1-tetradecanol as a filling agent, these nanofibers could have obvious body-temperature responsive properties. The fibers have obvious thermal energy management and thermochromic properties, good reversibility, and fluorescence. The encapsulation and fixing of PCTMs actualize their potential applications in thermochromic materials and sensors. These functional nanofibers provide new insight into the preparation of temperature sensors with good fluorescence signals and body-temperature calefactive materials with intelligent thermal energy absorption, retention, and release.

References

1. Gil, E. S.; Hudson, S. M. Prog Polym Sci 2004, 29, 1173.
2. Sun, T.; Feng, L.; Gao, X.; Jiang, L. Acc Chem Res 2005, 38, 644.
3. Pham, H. H.; Gourevich, I.; Oh, J. K.; Jonkman, J. E. N.; Kumacheva, E. Adv Mater 2004, 16, 516.
4. Lu, Y.; Liu, J. Acc Chem Res 2007, 40, 315.
5. Li, D.; Xia, Y. Adv Mater 2004, 16, 1151.
6. Zhang, Y.; Huang, Z.-M.; Xu, X.; Lim, C. T.; Ramakrishna, S. Chem Mater 2004, 16, 3406.
7. Teo, W. E.; Kotaki, M.; Mo, X. M.; Ramakrishna, S. Nanotechnology 2005, 16, 918.
8. Yu, J. H.; Fridrikh, S. V.; Rutledge, G. C. Adv Mater 2004, 16, 1562.
9. Dersh, R.; Steinhart, M.; Boudriot, U.; Greiner, A.; Wendorff, J. H. Polym Adv Technol 2005, 16, 276.
10. Jiang, H.; Hu, Y.; Li, Y.; Zhao, P.; Zhu, K.; Chen, W. J Controlled Release 2005, 108, 237.
11. Loscertales, I. G.; Barrero, A.; Guerrero, I.; Cortijo, R.; Marquez, M.; Ganan-Calvo, A. M. Science 2002, 295, 1695.
12. Díaz, J. E.; Barrero, A.; Márquez, M.; Loscertales, I. G. Adv Funct Mater 2006, 16, 2110.
13. Bognitzki, M.; Czado, W.; Frese, T.; Schaper, A.; Hellwig, M.; Steinhart, M.; Greiner, A.; Wendorff, J. H. Adv Mater 2001, 13, 70.
14. Patel, A. C.; Li, S. X.; Yuan, J. M.; Wei, Y. Nano Lett 2006, 6, 1042.
15. Lin, T.; Wang, H.; Wang, X. Adv Mater 2005, 17, 2699.
16. McCann, J. T.; Marquez, M.; Xia, Y. J Am Chem Soc 2006, 128, 1436.
17. Jiang, L.; Zhao, Y.; Zhai, J. Angew Chem Int Ed 2004, 43, 4338.
18. Zhao, Y.; Cao, X.; Jiang, L. J Am Chem Soc 2007, 129, 764.
19. Zhu, Y.; Zhang, J.; Zheng, Y.; Huang, Z.; Feng, L.; Jiang, L. Adv Funct Mater 2006, 16, 568.
20. Yoon, J.; Chae, S. K.; Kim, J.-M. J Am Chem Soc 2007, 129, 3038.
21. Roh, K.-H.; Martin, D. C.; Lahann, J. J Am Chem Soc 2006, 128, 6796.
22. Kuo, C.-C.; Lin, C.-H.; Chen, W.-C. Macromolecules 2007, 40, 6959.

23. Zalba, B.; Marin, J. M.; Cabeza, L. F.; Mehling, H. Appl Thermal Eng 2003, 23, 251.
24. Mulligan, J. C.; Colvin, D. P.; Bryant, Y. G. J Spacecraft Rockets 1996, 33, 278.
25. McCann, J. T.; Marquez, M.; Xia, Y. Nano Lett 2006, 6, 2868.
26. Burkinshaw, S. M.; Griffiths, J.; Towns, A. D. J Mater Chem 1998, 8, 2677.
27. Hirata, S.; Watanabe, T. Adv Mater 2006, 18, 2725.
28. Maclaren, D. C.; White, M. A. J Mater Sci 2005, 40, 669.
29. Koropchak, J. A.; Magnusson, L. E.; Heybroek, M.; Sadain, S.; Yang, X. H.; Anisimov, M. P. Adv Chromatogr 2000, 40, 275.
30. Gaudin, K.; Bailletn, A.; Chaminade, P. J Chromatogr A 2004, 1051, 43.
31. Bohren, C. F.; Huffman, D. B. Absorption and Scattering of Light by Small Particles; Wiley: New York, 1983.
32. van de Hulst, H. C. Light Scattering by Small Particles; Wiley: New York, 1957.
33. Li, F.; Yang, G.; He, Z. Laser J 2004, 25, 51.